CONNEXIN DISTRIBUTION AND OPTICAL MAPPING OF THE MAMMALIAN AV NODE.

Dermot James Kelly
Department of Physiology
McGill University, Montreal

October 2002

A thesis submitted to the Faculty of Graduate Studies and Research in partial fulfillment of the requirements of the degree of Masters' of Science.

Your file Votre référence
ISBN: 0-612-88228-4
Our file Notre référence
ISBN: 0-612-88228-4

TABLE OF CONTENTS

ABSTRACT

Atrioventricular (AV) nodal conduction and the pathways of propagation through the AV node have remained enigmatic. Histological and immunohistochemical studies have revealed distinct cellular regions within the AV node with varying distribution of specific ion channels. However, to date, there is little information concerning the pattern of localization of the gap junction proteins that mediate intercellular communication. The current immunohistochemical/confocal studies show a non-uniform distribution of three connexin isoforms (Cx 40, Cx 43 and Cx 45) within these cellular regions of the rat AV node with a marked transition from Cx 43 to Cx 40 at the compact node region. In addition, a high resolution mapping system coupled with extracellular recording electrodes was implemented during this study and has allowed for a macroscopic overview of the rabbit AV node. This approach revealed a marked delay in conduction at the area of the compact node. This information in association with the immunohistochemical studies may help to provide further insight into the mechanisms underlying the AV nodal delay.

RÉSUMÉ

La conduction nodale atrioventriculaire (AV) et les voies de la propagation à travers le noeud AV sont demeurées énigmatiques. Les études histologiques et immunohistochemical ont indiqué des régions cellulaires distinctes dans le noeud AV avec la distribution variable des voies spécifiques d'ion. Cependant, jusqu'ici, les études ont peu d'information au sujet du modèle de la localisation des protéines du jonction d'espace qui négocient la communication intercellulaire. Les études courantes d'immunohistochemical/confocal montrent une distribution non-uniforme des trois isoforms de connexin (Cx 40, Cx 43 et Cx 45) dans ces régions cellulaires du noeud AV de la rat avec une transition marquée de Cx de 43 à Cx 40 jusqu'à la région compacte de noeud. En outre, un système traçant de haute résolution couplé aux électrodes extracellulaires d'enregistrement a été mis en application pendant cette étude et a tenu compte d'une vue d'ensemble macroscopique du noeud AV de le lapin. Cette approche a indiqué un retarde marqué dans la conduction au secteur du noeud compact. Ces révélations en association avec les études immunohistochemical aidera à fournir une meilleure compréhension de les mécanismes sous-tendants le nodal AV retarde.

ACKNOWLEDGEMENTS

I would like to acknowledge the assistance that was given me by all persons in our lab: Johanne Ouellette, Kevin Petrecca, and Armin Akhavan. I would also like to extend my genuine gratefulness to Dr. Yoshihiko (Tiger) Nagai for all his help with the optical components of our apparatus and with the interpretation of the electrical and optical data. Special thanks are due to Dr. Leon Glass for his thoughtful discussions and aid with the optical and electrical data analysis. This research would not have been possible without the guidance and support that was extended to me by my supervisor, Dr. Alvin Shrier. His patience and insight provided me with the opportunity to undertake an extensive project and the background knowledge necessary to complete my goals. I owe him my utmost appreciation. Last, but not least, I would like to express my deepest gratitude to my parents for their love and faith in me.

CHAPTER 1

INTRODUCTION

BASIC ANATOMY OF THE HEART AND SPECIALIZED CONDUCTION SYSTEM

The mammalian heart is a complex structure possessing four distinct chambers, two atria and two ventricles. The right atrium receives deoxygenated blood from the systemic circulation and expels this fluid into the right ventricle. From here the blood is ejected and via the pulmonary artery enters the pulmonary circulation where it is to be oxygenated by the lungs. The left atrium receives the now freshly oxygenated blood from the pulmonary circulation and pushes this into the left ventricle, the larger of the two ventricles. From here the blood is pumped out into the systemic circulation via the aorta. In order to prevent the back flow of fluid from chamber to chamber upon contraction the heart is equipped with two atrioventricular valves. The tricuspid valve separates the right atrium from the left ventricle and the bicuspid valve the left atrium from the left ventricle. For the prevention of regurgitation of blood from the two main arteries back into the ventricles two more valves exist. The pulmonary valve separates the right ventricle from the pulmonary circulation and the aortic valve the left ventricle from the systemic circulation. In order to ensure that the maximum volume of blood is transferred from the atria to the ventricles, atrial contraction must precede ventricular contraction. This timing is very crucial and is coordinated by the specialized conducting tissues of the heart.

The normal site of impulse initiation (pacemaking) in the heart is found in a small area of specialized cardiomyocytes located at the junction between the superior vena cava and the right auricle. This area is known as the sinoatrial (SA) node. The mechanism behind this pacemaking activity remained unresolved until spontaneous diastolic depolarization was first observed with the use of microelectrode recording techniques[1].

The electrical wave, which is initiated by the SA node, traverses the atrial muscle causing the muscle fibres to contract in a synchronous fashion.

After atrial stimulation, the electrical impulse impinges on a small area of specialized cardiomyocytes known as the atrioventricular (AV) node, also referred to as the node of Tawara[2]. The AV node is the only normal anatomical and electrical link between the atria and the ventricles. The exact location, function and cellular characteristics of the AV node will be discussed later.

Once the impulse has passed through the AV node it is then conducted to the bundle of His, also know as the atrioventricular bundle. The bundle of His is made up of a collective bundle of cells located in the interventricular septum (IVS) which rapidly divide to form the left and right bundle branches. The left bundle branch combs the left surface of the IVS and the right bundle branch the right surface of the IVS. The bundles consist of specialized fibres, Purkinje fibres, which allow for the extremely fast conduction of the impulse in this area. The bundle branches fan out into a wide sheet under the endocardial mass of the ventricles and penetrate the myocardium allowing for the synchronous contraction of the large ventricular muscle masses and subsequently the projection of the blood, at high pressure, out of the ventricles and into the pulmonary and systemic circulations.

It should be mentioned that although the SA node is the primary pacemaking site of the normal heart, under pathophysiological conditions both the AV node[3] and even the Purkinje fibres[4] could display pacemaking activity. These properties are usually suppressed by the faster rhythm of the SA node[5] in the normal heart.

THE ATRIOVENTRICULAR NODE

It was in 1906 that Tawara[2] studied the hearts of many species of mammals and found essentially the same structure, in all, located at the anterior part of the base of the interatrial septum. He described a spindle-shaped compact network of cells that were connected by fibres. It was this characteristic that led him to call this network "Knoten" ("node"). Apart from Tawara's main hypothesis, that the AV node serves as the only electrical link between the atria and the ventricles, three other unique characteristics for this region exist. 1) The existence of the AV node causes a slow conduction delay allowing for the coordinated activation of the atria and the ventricles. 2) The AV node also acts as a protective mechanism blocking premature impulses originating in the atria and preventing them from activating the ventricular muscle mass, which could cause irregular heart rhythms. 3) In the event of a block between the atria and the AV node or SA nodal failure, the AV node can act as a subsidiary pacemaker to the ventricles.

Although there are many different views as to the exact morphological location of the AV node, the general consensus is as follows. The AV node is located within a triangular region referred to as the triangle of Koch[6]. The apex of the triangle is the formed by the membranous septum. The attachment of the septal tricuspid leaflet forms the inferior border and the superior border is bounded by the tendon of Todaro, a strand of fibrous tissue extending from the central fibrous body to the sinus septum above the ostium of the coronary sinus.

In the rabbit[7] and rat[8] heart the AV nodal area can be divided into two separate regions. The open node, posterior portion of the node, wherein the cells in this region make open contact with the surrounding cells of the atria and the anterior closed node.

The closed node is enveloped by a collar of connective tissue that is formed by the annulus fibrosus and an extension from the central fibrous body[7]. Within the boundaries of the AV node three distinct cellular regions exist: 1) the transitional cells, 2) the midnodal cells and 3) the lower nodal cells.

The Transitional Cells

The transitional cells are located in the proximal region of the AV node and occupy a significant amount of the cellular area within this region. They can be distinguished from other atrial cells by their smaller size and lighter colour. For the most part, they are arranged in a parallel fashion separated from their neighbours by strands of connective tissue. Due to this gradual transition from working atrial muscle to specialised tissue there has been great controversy as to where the atrium ends and the AV node begins[9]. Three different groups of transitional cells have been described within the rabbit AV node[7,9,10].

The first group, the posterior group, is in contact with the atrial myocardium just below and in back of the coronary sinus. The second group, the middle group, is located just anterior to the ostium of the coronary sinus and is in contact with the atrial cells of the sinus septum. The cells of the middle group also make contact with the deeper layers of the left side of the interatrial septum. The last group, the anterior group, makes contact with the atrial myocardium near the ostium of the coronary sinus and overlay the AV node from the area just below the tendon of Todaro to the annulus fibrosus.

There is another "group" of transitional cells that should be mentioned. They are the circumferential transitional cells. These cells have a more irregular arrangement, than their counterparts, and are located around the area of the compact node[11].

The Midnodal Cells

The transitional cells all merge at the entrance of the enclosed node and surround a small knot of tightly packed cells. These cells are commonly referred to as midnodal cells and the area with which they occupy, the compact node. The compact node, as mentioned previously, is located in the area of the enclosed node and is surrounded by connective tissue almost excluding it from the other cells in this region. This area is of vital importance as it is believed to be the pacemaking site[12,13] of the AV node as well as constituting for the majority of the AV nodal delay[14].

Midnodal cells are the smallest cells of the AV node and unlike the transitional cells, they are separated by very little connective tissue. They are ovoid and spindle shaped in appearance and contain very few myofibrils[9]. The midnodal cells are bordered superiorly and posteriorly by the transitional cells as well as inferiorly by another group of cells known as the lower nodal cells.

The Lower Nodal Cells

The lower nodal cells are elongated and are smaller than atrial cells. Fibrous tissue septa separate individual cell groups into bundles. These bundles, also known as the lower nodal cell tract, extend throughout the entire length of the AV node running parallel to the AV ring. Within the area of the open node, no contact between transitional and lower nodal cells is apparent. The lower nodal cell tract is very thin at the beginning of the open node, however, the diameter of the tract increases and reaches a maximum as it penetrates the closed node. It is here that the lower nodal cells are in contact with the transitional cells and are in close proximity to the midnodal cells.

GAP JUNCTIONS

The specialized myocytes of the conduction systems share with the working myocardium four key elements: 1) contraction, 2) electrical excitability, 3) intercellular conduction and 4) electromechanical coupling. It is the arrangement of these particular myocyte populations that allows for the coordinated activation of the heart. Sequential contraction of the cardiac chambers is stimulated by the orderly spread of action potentials between all the constituent cardiac muscle cells of the myocardium. Intercalated disks occur not only at the ends of the main body of the cell but also along its length. In turn, each myocyte is linked to an average of 9 to 12 neighbours in the ventricle. It has long been known that the conduction of action potentials between the myocytes depends upon a specific type of intercellular junction, the gap junction.

The gap junction was originally characterized by its appearance in thin-section electron micrographs as a pair of membranes of variable area separated by a 2-nm "gap"[15]. The gap junction is a highly specialized organelle consisting of clustered channels whose unique design permits the direct intercellular exchange of ions and molecules through central aqueous pores[16]. These intercellular channels allow for a unique form of communication between adjacent cells in that the exchange of molecules occurs without secretion into the extracellular space. These channels are more complex than other ion channels because a complete cell-to-cell channel spans two plasma membranes. This results from the association of two half channels, or connexons, contributed separately by each of the two neighbouring cells[16].

Each connexon is comprised of six protein subunits deemed connexins. The first connexin (Cx) cDNA was cloned in 1986[17] and, to date, 14 other members of the

connexin family have been cloned in rodents. Each connexin contains four transmembrane (M1-M4), two extracellular (E1-E2) and three cytoplasmic regions[18]. Both extracellular loops contain three cysteine residues in a characteristically conserved sequence (CX_6CX_3C in E1 and CX_4CX_5C in E2)[19]. The extracellular interaction of the two connexon hemichannels, from adjacent cells, is believed to occur across the cysteine residues. This interaction forms the direct communication link between the cytoplasms of the two cells.

In the AV node, where conduction is slow to ensure sequential activation of the atria and ventricles, gap junctions are small and sparse, whereas in the Purkinje fibres and working myocardium, where excitation is rapid, gap junctions are abundant and larger in size. The expression of three unique connexin proteins has been identified in the cardiomyocytes of the AV node. They are Cx 40, Cx 43 and Cx 45.

Connexin 40 (Cx 40)

Cx 40 is a member of the family of gap junction proteins. Its mRNA is abundant in lung and is also present in the mammalian heart. Double-labeling experiments carried out with lung sections using anti-factor VIII and anti-Cx 40 antibodies suggest that Cx 40 is expressed in blood vessel endothelial cells[20]. Cx 40 was found to be expressed in rat heart ventricular tissue, but its expression is restricted to certain regions: 1) the upper apex of the interventricular septum (IVS), corresponding with the bundle of His, 2) two regions extending along the IVS on either side, corresponding with the bundle branches and 3) the false tendons joining the IVS to the lateral ventricular walls, containing the Purkinje fibres[20]. Cx 40 is expressed in the myocytes of the specialized conduction system of the heart including the midnodal region of the AV node. It was once believed

to be the only connexin protein associated with this particular region as previous experiments showed that Cx 43 was not detected in the atrioventicular node, the bundle of His or the proximal part of the bundle branches in rat[21,22]. However, our study shows that Cx 40 and Cx 43 are closely associated with each other in the area of the atrioventricular node and the distal part of the bundle branches in rat heart. These differences are most likely attributed to our more accurate histological sectioning of the AV node.

The presence of both Cx 40 and Cx 43 in these particular regions of the conduction system could be helpful in the regulation of the conduction velocity. The unitary conductance of Cx 43 junctional channels of myocytes has been estimated to be 40 to 60 picosiemens[23]. HeLa cells transfected with Cx 40 cDNA have shown the unitary conductance of Cx 40 channels to be approximately 150 picosiemens[24]. Ignoring all other factors, this evidence shows that cells connected by Cx 40 channels should conduct action potentials much faster than those connected by Cx 43 channels. The difference in the unitary conductance properties of these channels may be a contributing factor in the AV nodal delay due to their close association with one another.

Connexin 43 (Cx 43)

Cx 43 is the major gap junction protein in the adult rat heart. Its abundance in the working myocardium of the heart is clearly evident using immunolabeling experiments and confocal laser microscopy. Even though Cx 43 expression is seen throughout the working myocardium of the atria and ventricles, as previously mentioned it had remained undetected in the AV node, bundle of His and proximal regions of the bundle branches of the rat heart[21,22]. Its expression in these particular regions is very complex. Cx 43 is

widely expressed in the myocardium of the basal part of the IVS that is continuous with the free wall of the ventricle. However, its expression is diminished in the subendocardial sheet that is continuous with the atrioventricular canal (i.e. the proximal region of the specialised conduction system).

A transitional zone between the crista terminalis and the periphery of the AV node was detected in which Cx 43 expression emerged[25]. The boundary between Cx 43 positive and Cx 43 negative tissue in the area of the AV node, more particularly the midnodal region is quite apparent. However, it is clear that some Cx 43 positive atrial myocytes do penetrate the nodal region.

Connexin 45 (Cx 45)

Cx 45 has been one of the more difficult gap junction proteins in determining its distribution within the mammalian heart. Previous reports have concluded that Cx 45 was widely distributed in the working ventricular myocytes closely associated with Cx 43. However, these studies involved the use of a commercially available antibody, which was inhibited by a six-amino acid peptide matching part of the Cx 43 sequence, indicating cross-reactivity[26]. This same group[26] demonstrated, with the use of a personally developed antibody, that Cx 45 positive zones were consistently restricted to the endocardial surface, where components of the conduction system are localised.

As the myocytes of the conduction system have characteristically expressed Cx 40, these experiments demonstrated that Cx 40 and Cx 45 colocalize to the same intercalated disk. However, Cx 45 was not restricted to only Cx 40 positive zones. These findings may draw to the conclusion that Cx 45 acts as a mediator between Cx 43 and Cx 40 in otherwise incompatible zones.

ELECTROPHYSIOLOGY

As previously mentioned the AV node has been divided histologically into three distinct cellular regions. However, originally the AV node was divided into three electrophysiological zones displaying different properties including unique activation times and transmembrane electrical characteristics[14]. There has been a definite correlation between the three cellular regions of the AV node defined in histological studies[9] and the three electrophysiological regions defined by Paes de Carvalho and de Almeida[14].

The first of these regions is the Atrial-Nodal (AN) zone. This zone represents the transitional area between those cells of the atrium and the cells of the midnodal region of the AV node. The AN zone represents electrophysiologically the transitional cells of the AV node. In this particular region there is a gradual decrease in the upstroke and conduction velocity as the electrodes are positioned further from the atrium and closer to the Nodal (N) region of the AV node[27].

It is the N zone in which the maximal decrease in conduction velocity and upstroke velocity is noted[27]. The pacemaking activity of the AV node is believed to lie within this particular region of the AV node. It is this N zone that correlates electrophysiologically with the midnodal cells of the AV node. It is also speculated that the major participant in the AV nodal delay occurs between the transition from the N zone to the Nodal-His (NH) region of the AV node[27].

The NH zone of the AV node has similar properties as to that of the AN zone with respect to the fact that they both demarcate transitional areas. The NH cells demonstrate electrophysiological properties of transition cells from those with N characteristics to

those with His characteristics[27]. These cells have an increased upstroke and conduction velocity with respect to N cells, however, not as marked an increase as the AN cells. It is the NH zone that correlates electrophysiologically with the lower nodal cells.

This particular study[27] was performed using a protocol whereby a periodic premature stimulation of the atrium directly correlated the nodal conduction and refractory properties with the changes in the activation of the various cells of the AV node. This protocol is an invaluable tool for measuring these properties and was used in our study in conjunction with an optical camera to measure and visualize the area of AV nodal delay.

OPTICAL MAPPING

The application of potential-sensitive molecular probes and optical imaging techniques in the mapping of cellular structures has become increasingly more common. Specifically, this tool is being used extensively in studies of a cardiac nature. However, due to the limitations of the potentially sensitive dyes these techniques have been mainly focused on two-dimensionally flat cellular cultures[28].

The AV node of the rabbit is located directly below the endocardial surface of the right atrium between the ostium of the coronary sinus and the IVS. Through histological studies the depth of the AV node of the rabbit is believed to be no more than 500 μm[11]. Therefore, staining of this area with voltage-sensitive dyes, such as 4-[β-[2-(di-*n*-butylamino)-6-naphthyl]vinyl]pyridinium (di-4-ANEPPS), may aid in providing a three-dimensional mapping of the AV node when used in unison with an optical recording device.

With the use of compound lenses, easily purchased in the consumer market, we have constructed a tandem-lens system capable of aiding us in the three-dimensional mapping of the AV node. The tandem-lens system is based on the principle of two lenses set to infinite focus that are placed face-to-face and the object/image conjugates are then located at the back focal planes of the respective lenses[29] which is where the cooled charged coupled (CCD) optical recording device is located. This system incorporates epi-illumination and a 40 mm working distance for imaging wide fields in the range of 1.5-20mm in diameter[29], a perfect fit for the rabbit AV node. However, one limitation does exist in that previous optical studies of the rabbit AV node[30,31,32] have suggested that the optical recordings may carry signatures of electrical activity from several layers of the area.

CHAPTER 2

MATERIALS AND METHODS

Tissue Processing

Female Sprague-Dawley rats, weighing approximately 225 g - 250 g, were killed by cervical dislocation. A midline thoracotomy was performed and the hearts were rapidly removed. The hearts were placed in a tissue bath perfused with Tyrode solution (composition mM): 121 NaCl, 5 KCl, 15 $NaHCO_3$, 1 Na_2HPO_4, 2.8 Na acetate, 1 $MgCl_2$, 2.2 $CaCl_2$ and 5.5 glucose) and gassed with 95 % 0_2 and 5 % CO_2. The dissection was performed and the preparation, containing most of the right atrium, the annulus fibrosus, the interatrial septum, the atrioventricular region and the upper portion of the interventricular septum was immediately frozen in isopentane cooled to – 80^0C. The preparation was then trimmed into a small block containing the interatrial septum, the upper portion of the interventricular septum and the ostium of the coronary sinus. The blocks were oriented to allow sectioning at right angles to the annulus fibrosus in the frontal plane. They were then mounted on a cryostat tissue holder using Histo Prep (Fisher Scientific, Ontario, Canada) and placed on a rapid freeze stage of a Microm cryostat (Carl Zeiss). The entire AV node, bundle of His and proximal bundle branches were cut into 12-mm sections. Each section was collected and processed for histological and immunohistochemical staining. In total, six hearts were sectioned.

Histology

All sections were collected on glass slides and every 5^{th} section was used for histological processing. The slides were dried at room temperature for 30 minutes and then incubated in Bouin's solution for 15 minutes at 56^0C. Sections were subsequently washed in running tap water and stained using a modified Masson's trichrome technique.

The slides were then washed in 1 % acetic acid for 2 minutes, dehydrated in increasing concentrations of ethyl alcohol, cleared in xylene and mounted. Sections were examined using a light microscope and then photographed on Kodak film. Blue staining indicates connective tissue and red staining indicates cardiomyocytes.

Antibodies

Cx 40 antibody (David Paul, Harvard Medical School) was prepared in rabbit against a GST fusion protein containing most of the unique C-terminal regions of rat Cx 40. The antibody was affinity purified against the fusion protein. Cx 43 antibody (Chemicon International Inc) is a synthetic peptide, prepared in mouse, corresponding to positions 252-270 of the native sequence from rat cardiac Cx 43. Two Cx 45 antibodies (Chemicon International Inc) were used in the course of this study. Both antibodies are synthetic peptides corresponding to positions 354-367 of human Cx 45 (Chemicon International Inc). Cx 45A (MAB 3100) and Cx 45B (MAB 3101) are different clones of monoclonal antibodies that were raised in mouse.

Immunocytochemistry

Human embryonic kidney (HEK) cells were cultured in αMEM (Gibco-BRL) supplemented with 10 % FBS (100 mL) and 1 % penicillin/streptomycin (10 mL, Gibco-BRL). Cells were plated onto 4-12 mm diameter glass coverslips in 6 well plates and grown until approximately 80 % confluent. cDNAs encoding mouse Cx 40 (David Paul, Harvard Medical School), human Cx 43 and mouse Cx 45 (both provided by Dale Laird, University of Western Ontario) were ligated into the pBK-CMV expression vector (Stratagene). Cells were transfected using 3 μL of Lipofectamine (Gibco-BRL) and 1 μg

of the appropriate cDNA per mL of Opti-MEM (Gibco-BRL) and incubated for a 5 hour period. The transfection medium was subsequently removed and the cells were re-incubated with αMEM for 48 hours.

Cells plated on coverslips were fixed, at room temperature, in 2 % paraformaldehyde for 30 minutes followed by 3 2-minute washes in PBS. Cells were then incubated for 30 minutes in PBS containing 0.2 % Triton X-100 and 0.5 % BSA. Cells were subsequently washed in PBS, 3 10-minute washes, followed by a 1-hour incubation with the appropriately diluted primary antisera [Cx 40 (1:100), Cx 43 (1:200) and Cx 45 A, B (1:200)]. This was followed by 3 10 minute washes in PBS and then a 1 hour incubation with appropriately diluted secondary antisera; Cyanine [Cy3 (1:100)]-conjugated goat antirabbit IgG (Bio/Can Scientific) and Oregon Green 488 [OG (1:100)]-conjugated goat antimouse IgG (Molecular Probes). This incubation was followed by 3 10 minute washes in PBS. The cells were then mounted with Immuno Fluore (ICN, Canada).

Immunohistochemistry

All the immunolabelling was performed on unfixed tissue. Serial cryosections were double labeled for Cx 40 and Cx 43 and for Cx 40 and Cx 45. The 12 mm cryostat sections were air-dried at room temperature for 30 minutes. The sections were then incubated in PBS, containing 0.2 % Triton X-100 and 0.5 % BSA, for 30 minutes. Sections were subsequently rinsed in PBS and incubated for 1.5 hours with appropriately diluted primary antisera [Cx 40 (1:100), Cx 43 (1:200) and Cx 45A, (1:200)]. Following the 1.5 hour incubation the sections were washed 3 times for 10 minutes in PBS and then incubated for another 1.5 hours in appropriately diluted secondary antisera; Cyanine [Cy3

(1:100)]-conjugated goat antirabbit IgG (Bio/Can Scientific) and Oregon Green 488 [OG (1:100)]-conjugated goat antimouse IgG (Molecular Probes). These incubations were followed by 3 10-minute washes in PBS. The second labeling was then performed following the same protocol as for that of the first, excluding the incubation period with Triton X-100 and BSA. The preparations were mounted with Immuno Fluore (ICN, Canada). Specificity controls included the omission of the primary antisera.

All imaging (immunocyto- and immunohisto-) was performed using a BioRad MicroRadiance inverted confocal microscope. Exciting the samples with a 488 and a 540 nm line from an argon-krypton laser imaged the Cy3 and OG-conjugated secondary antibodies respectively. The resulting fluorescence was collected on a photomultiplier after passage through FT 510 and BP 515-540 filter sets, for the Cy3, and FT 510 and LP 570 filter sets, for the OG. Optical sections were taken using a 25 X, 0.8 NA (optical thickness = 3.1 mm) objective or a 63 X, 1.4 NA (optical thickness = 1.0 mm) objective.

Electrophysiology

The experiments were performed on isolated female New Zealand White rabbits, weighing approximately 1.8 kg – 2.5 kg. The animals are first anaesthetized with an intramuscular injection containing a mixture of ketamine (70 mg/kg) and xylazine (10 mg/kg). Hepalean (1000 units/ml) is injected intravenously to prevent blood coagulation. A mid-line thoracotomy is performed and the heart is quickly removed and dissected. The preparation, containing most of the right atrium, the annulus fibrosus, the interatrial septum, the atrioventricular region and the upper portion of the interventricular septum is placed in a tissue bath and pinned in its proper orientation. The heart is then superfused with oxygenated (95 % O_2 and 5 % CO_2) Tyrode solution (mM composition same as

previously mentioned) warmed to 37^0C and at a pH of ~7.4. The temperature of the Tyrode solution is maintained via a feedback system consisting of an electrical jacket mounted on the side of the tissue bath, a temperature controller (NBD) and a temperature probe (Yellow Springs Instruments). A 2.0 L volume of Tyrode solution is continuously reoxygenated and recirculated at a flow rate of 110 mL/min.

A bipolar Teflon coated Pt-Ir stimulation electrode is then positioned just superior to the ostium of the coronary sinus on the crista terminalis, near the area of the sinus node, to allow for entrainment of the preparation. Bipolar Teflon coated Ag-$AgCl_2$ recording electrodes were placed on the lower portion of the interatrial septum and at the region of the bundle of His. Electrograms were amplified (Grass P5 A.C. Pre-Amplifiers), sent to an oscilloscope (Tektronix 5110) and detected by a data acquisition program at a sampling rate of 1 kHz.

The conduction and refractory properties of the AV node were studied using periodic premature stimulations of the right atrium. The rectangular voltage pulses have twice-threshold amplitude and 8 msec duration. A decremental premature pulse is delivered to the preparation, after every 20^{th} basic pacing interval, in shorter coupling-intervals (i.e. 20, 10, 5 and 2 msec). The basic pacing interval corresponds to a cycle length that is 30 msec shorter than the intrinsic SA nodal cycle length of the preparation. AV nodal responses to the premature protocol are presented as a recovery curve. Conventional notations were used to designate the beats obtained during the premature pacing protocol. The stimulation, atrial and His responses are represented by S, A and H respectively. The subscripts 1 and 2 represent the basic and premature beats respectively.

Optics

The same animal preparation used for the electrophysiologogical studies is used for the optical recordings. A 20.8 mM stock solution of the voltage-sensitive dye, di-4-ANEPPS (Molecular Probes), is prepared with the addition of 500 μL of the solvent dimethyl sulfoxide (DMSO) and stored in an uv-sensitive dessicator at room temperature. The final staining solution is prepared just prior to the dissection. 180 μL of the stock solution is added to 75 mL of warmed Tyrode solution, yielding a final concentration of 50 μM, and added to an isolated chamber within the tissue bath that contains the preparation. The solution is oxygenated and the preparation is superfused with this solution for 25 minutes. Following the staining procedure, the solution is removed and the preparation is once again superfused with Tyrode solution. To prevent contraction-induced artifacts of the optical recordings, butanedione monoxime (BDM) 10 mM is added to the Tyrode solution.

Light from a 250 W quartz-tungsten halogen DC light source (Oriel Corp) is passed through a liquid cooled infra-red filter (Oriel Corp), a 485 $\pm$ 35 nm excitation filter (Omega Optical) and is then directed at the surface of the preparation through a trifurcated fibre optic bundle (Omega Optical). The emitted light passes through a 610 nm long pass filter (Omega Optical), a tandem-lens system, consisting of a Nikon 35 mm AF Nikkor lens and a C-mounted lens, and is collected by a cooled charged coupled device (CCD) camera (Princeton Instruments). The data is then passed to a ST-138 CCD camera controller (Princeton Instruments), which contains a built in A/D converter, and then to the computer. The data is then visualized using Winview 32 (Princeton Instruments), a visual data acquisition program, and stored for further analysis. The

sampling is performed at a rate of 100 frames/sec. Both the electrophysiological and the imaging system were self-designed and built during the course of this study.

CHAPTER 3

RESULTS

Histology

The mammalian AV node is located anterior to the ostium of the coronary sinus and posterior to the IAS with the inferior portion bordering at the attachment of the septal tricuspid leaflet. As mentioned previously, the AV node is divided into two distinct regions, the posterior open nodal region and the anterior closed nodal region. Each region consists of different cellular zones with the defining factor being that the closed node is encased in a fibrous capsule (Fig 1 B).

The closed node extends anteriorly and is continuous with the bundle of His. The bundle of His runs alongside the central fibrous body before penetrating through the annulus fibrosus into the IVS where it divides into the bundle branches (Fig 1 C, D). The open node is bordered anteriorly by the closed node, inferiorly by the annulus fibrosus and superficially by the atrial myocardium (Fig 1 A).

Within the AV node there are three distinct cellular types associated with their own particular regions. The first of these are the transitional cells (Fig 1 A). These cells are a continuation of the atrial myocardium, however, they differ from atrial cells in that they are smaller in size and not quite as tightly packed together, separated from each other by connective tissue. For the most part, these cells were found only in the open node. However, within the closed node circumferential transitional cells (Fig 1 B) are apparent. These cells are similar in shape and size to the transitional cells, however, these particular cells are also seen sporadically within the fibrous capsule that surrounds the mid-nodal cells.

Figure 1

Frontal sections of the rat AV node, bundle of His and bundle branches stretching from posterior to anterior. Blue staining indicates connective tissue while red staining indicates myocardial cells. A) Section taken at the boundary between the open and the closed nodes. B) Section taken at the central portion of the closed node. C) Section taken at the anterior portion of the closed node just prior to penetration by the bundle of His, BHIS. D) Section taken through the BHIS showing the left and right bundle branches, BB. AM, atrial myocardium; VM, ventricular myocardium; TC, transitional cells; LNC, lower nodal cells; CTC, circumferential transitional cells; MNC, mid-nodal cells; FC, fibrous capsule. The bar scale is set at 250 μm.

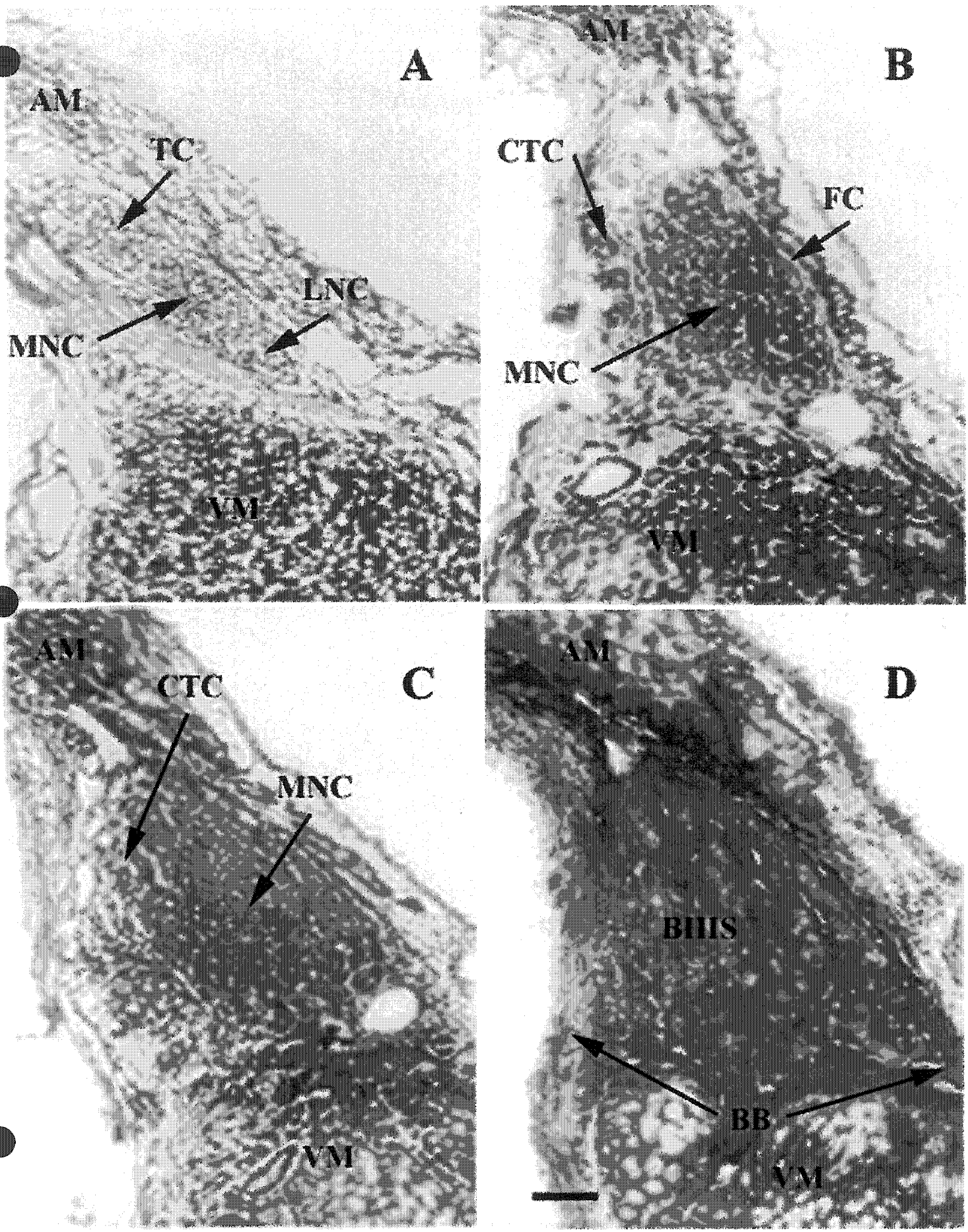
A
AM
TC
LNC
MNC
VM
B
AM
CTC
FC
MNC
VM
C
AM
CTC
MNC
VM
D
AM
BHIS
BB
VM

Having penetrated the anterior portion of the closed node, the central transitional cells come together to form a tight bundle of cells. These cells are known as the midnodal cells (Fig 1 B) and are distinct in their cellular properties. These cells are spherical in shape and much smaller in size that their counterparts, the transitional and lower nodal cells.

The lower nodal cells (Fig 1 A) run parallel to the annulus fibrosus through the open node and inferiorly to the midnodal cells through the entire portion of the closed node. These cells are much larger than the transitional and midnodal cells. It was also evident that as we extended our sections anteriorly the lower nodal cells were continuous with those cells of the bundle of His.

Immunocytochemistry

cDNAs encoding mouse Cx 40, human Cx 43 and mouse Cx 45 were transfected and transiently expressed in HEK 293 cells. The cells were then incubated in appropriately diluted secondary antisera and fluorescence confocal microscopy was used to determine the affinity of each of the connexin antibodies for their respective cDNAs as well as the potential for antibody crossreactivity.

HEK 293 cells transiently transfected with cDNA for mouse Cx 40 and labeled with Cx 40 antibody showed localization at the surface membrane (Fig 2A). Cells transfected with cDNA for human Cx 43 and labeled with Cx 40 antibody showed no signs of localization (Fig 2B). In contrast, cells transfected with Cx 45 and labeled with Cx 40 antibody (Fig 2C, D) did show signs of surface membrane localization.

Figure 2

A) Surface membrane localization (arrow) of Cx 40 in Cx 40 transiently transfected HEK 293 cells. B) No signs of cross-reactivity between Cx 40 antibody and Cx 43 transiently transfected cells. C, D) Possible cross-reactivity of Cx 40 antibody and Cx 45 transiently transfected cells. E) No labeling in untransfected cells. The bar scale is set at 50 μm.

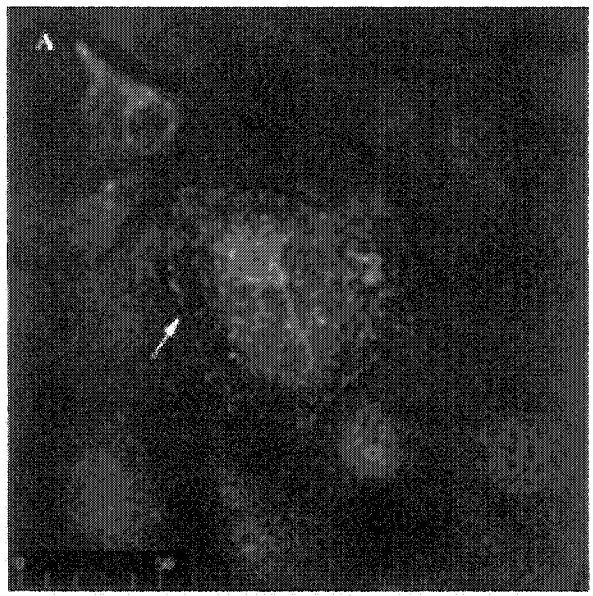
A

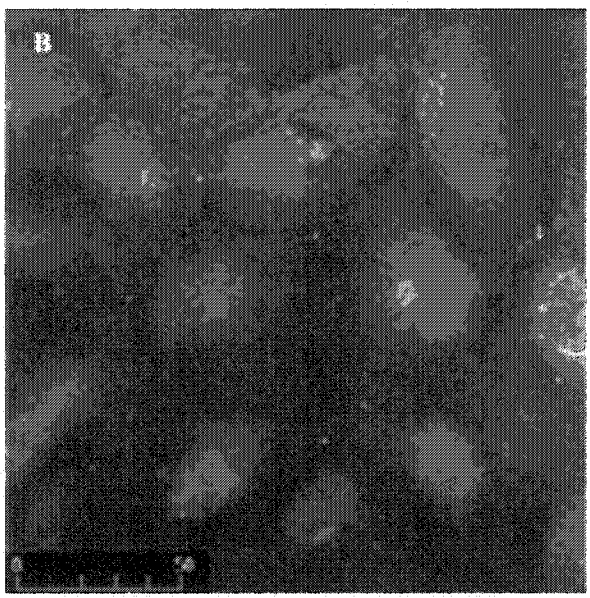
B

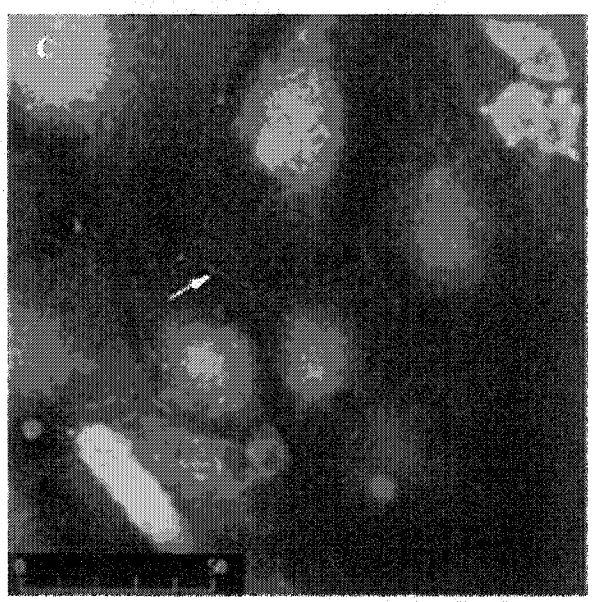
C

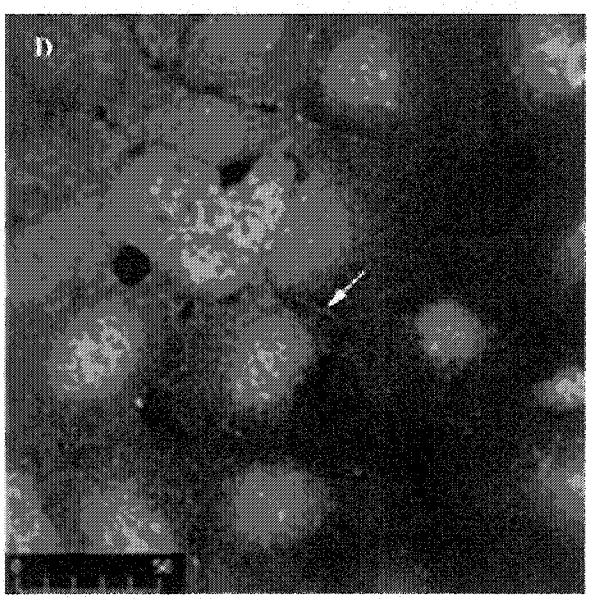
D

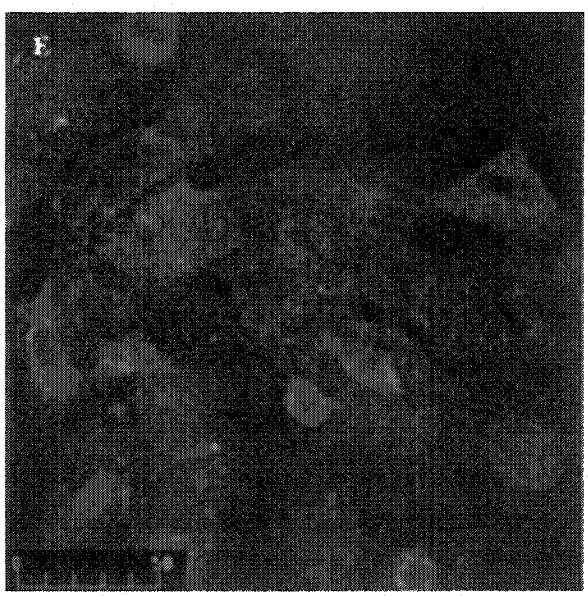
F

However, the purity of the Cx 45 encoding cDNA was in question as previous studies have raised concerns[33].

HEK 293 cells transiently transfected with cDNA for human Cx 43 and labeled with Cx 43 antibody showed localization at the surface membrane (Fig 3B). As with Cx 40, there were no signs of cross-reactivity between cells transiently transfected with Cx 43 and labeled with Cx 40 antibody (Fig 3A). Once again, the cDNA encoding for Cx 45 did show signs of cross-reactivity with the Cx 43 antibody (Fig 3C, D).

HEK 293 cells transiently transfected with cDNA for mouse Cx 45 and labeled with Cx 45A and Cx 45B antibodies showed localization at the surface membranes (Fig 4C, D respectively). However, there were no signs of cross-reactivity between Cx 40 and Cx 43 transiently transfected cells labeled with Cx 45A antibody (Fig 4A, B respectively). The commercially available Cx 45A antibody was used throughout the rest of the study due to the higher affinity for the Cx 45 cDNA (Fig 4C).

Although the surface localization of the connexins is the main focus of this experiment, it is common to have over-expression that often shows up as an overloading of the endoplasmic reticulum (ER) and Golgi apparatus systems. This leads to heavy peri-nuclear staining. However, when similar staining is performed in intact tissue these patterns are not normally observed.

Immunohistochemistry

Low magnification confocal microscopy, collected under identical conditions to allow for a relative comparison, demonstrates a pattern to the connexin protein distribution within the area of the AV node (Fig 5). The immunofluorescence levels between different tissue regions demarcates a distinct boundary between Cx 40 and Cx

43. The area of the transitional cells (Fig 5, first row) demonstrates a high level of the Cx 43 protein similar to those levels found in the surrounding atrial and ventricular myocardium. In contrast, no levels of Cx 40 immunofluorescence were present in the transitional cell region.

Figure 3

A) No signs of cross-reactivity between Cx 43 antibody and Cx 40 transiently transfected HEK 293 cells. B) Surface membrane localization (arrows) of Cx 43 in Cx 43 transiently transfected cells. C, D) Possible cross-reactivity of Cx 43 antibody and Cx 45 transiently transfected cells. E) No labeling in untransfected cells. The bar scale is set at 50 μm.

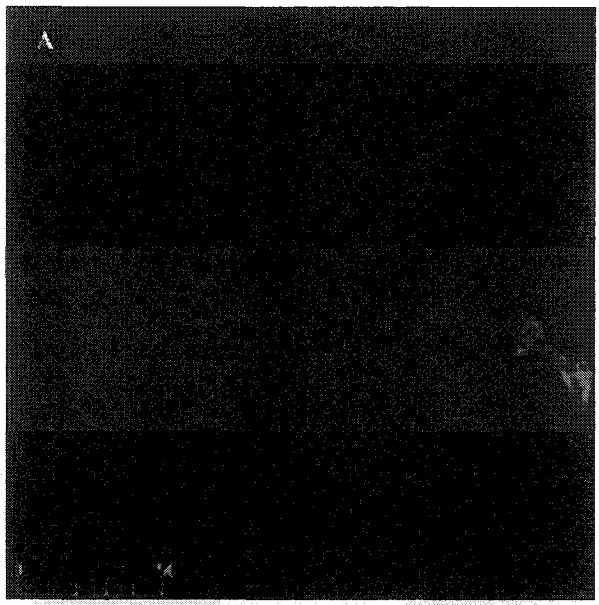
A

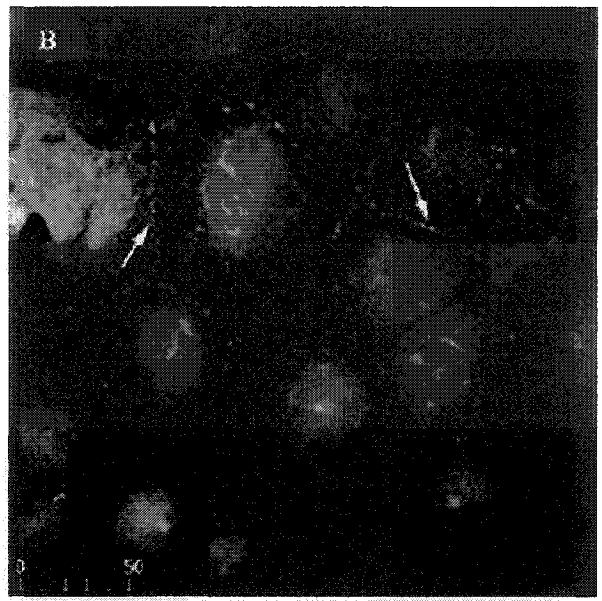
B

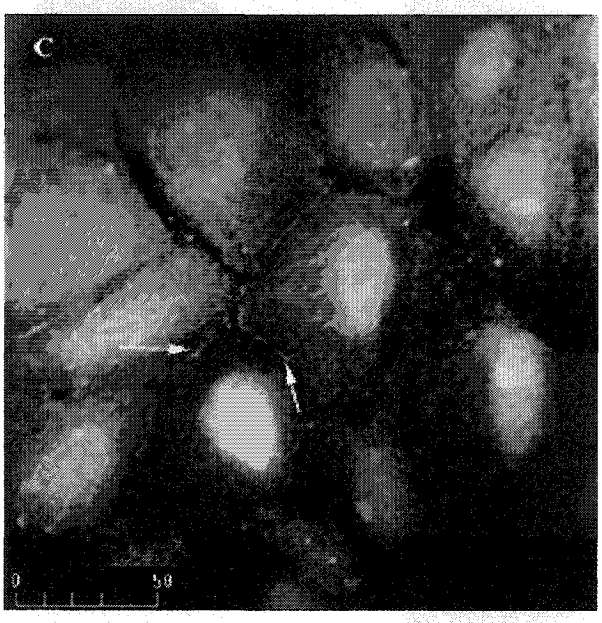
C

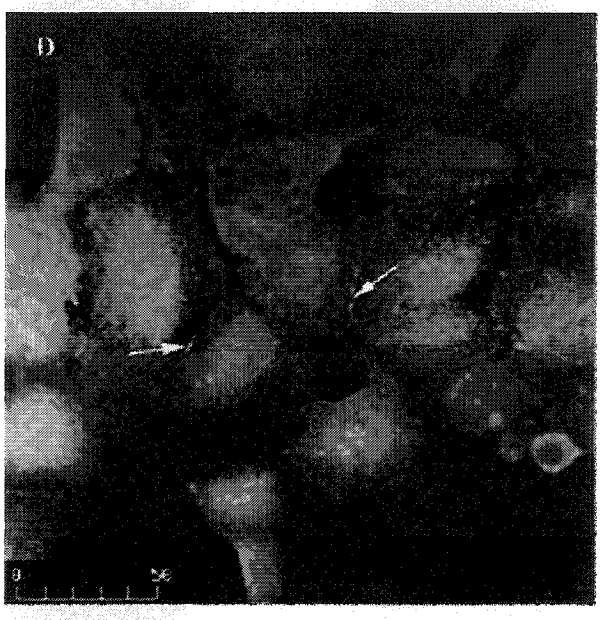
D

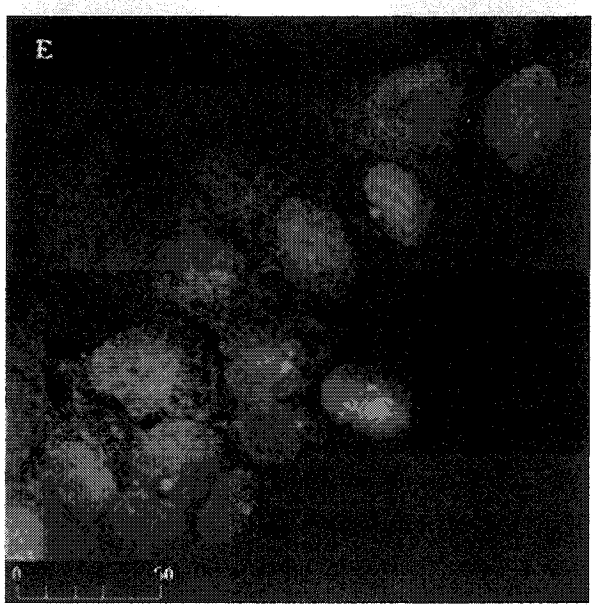
E

Figure 4

A) No signs of cross-reactivity between Cx 45A antibody and Cx 40 transiently transfected HEK 293 cells. B) No signs of cross-reactivity between Cx 45A antibody and Cx 43 transiently transfected cells. C) Surface membrane localization (arrows) of Cx 45 in Cx 45 transiently transfected cells labeled with Cx 45A antibody. D) Surface membrane localization (arrows) of Cx 45 in Cx 45 transiently transfected cells labeled with Cx 45B antibody. E) No labeling in untransfected cells. The bar scale is set at 50 μm.

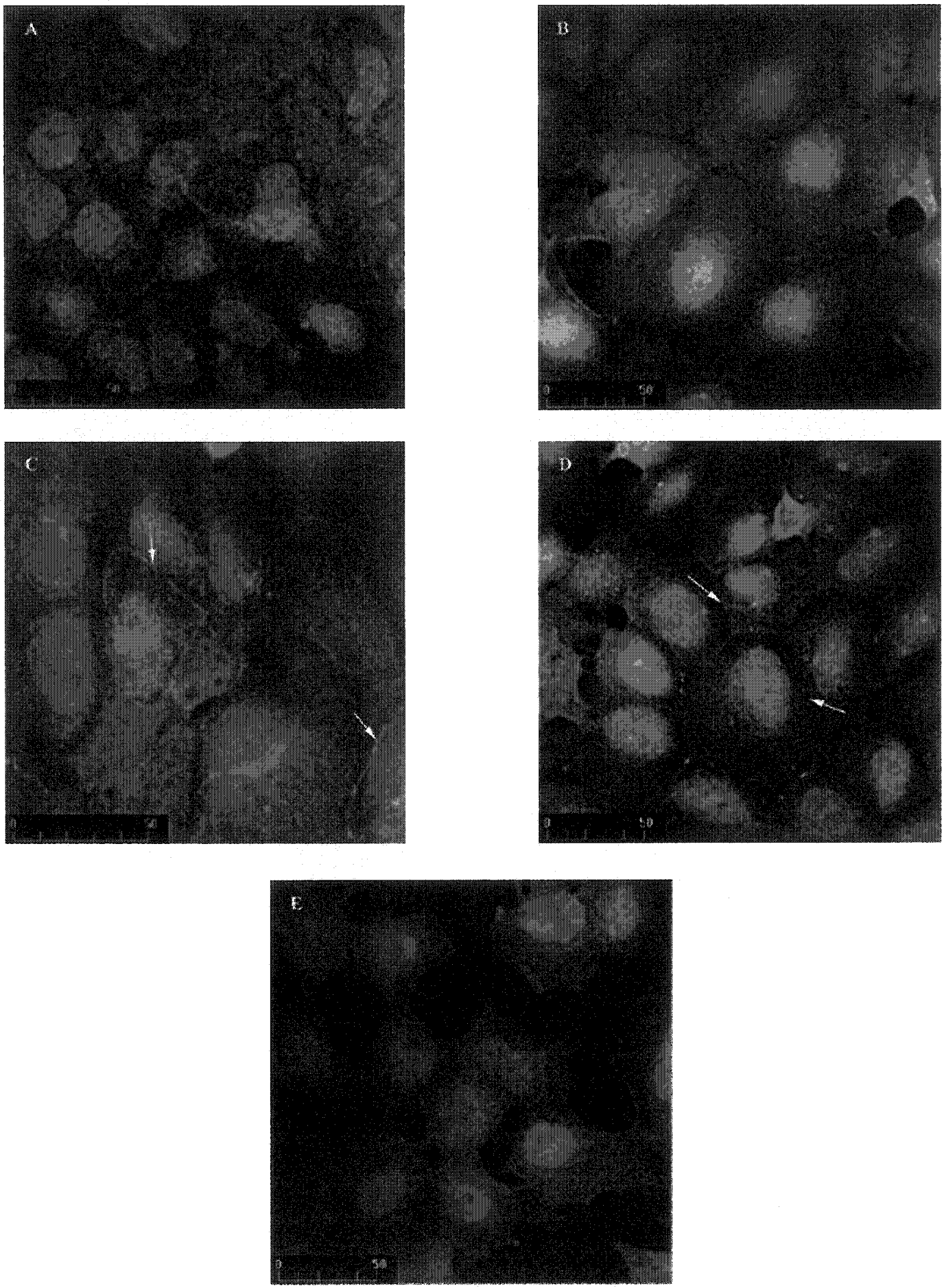
A
B
C
D
E

Figure 5

All sections were in the frontal plane tracing the course of the AV node from posterior to anterior. Row 1: Sectional slides of the transitional cell (TC) region demonstrating no levels of Cx 40 and high levels of Cx 43. Row 2: Sectional slides of the posterior mid nodal cell (PMNC) region demonstrating no levels of Cx 43 within the boundaries of the packed mid node (^) and minimal levels within the circumferential transitional cells (*); whereas high levels of Cx 40 are present within the packed mid node. Row 3: Sectional slides of the distal mid nodal cell (DMNC) region demonstrating once again no levels of Cx 43 and high levels of Cx 40 within the packed mid node. Row 4: Sectional slides of the bundle of His (BHis) demonstrating high levels of Cx 40 and no levels of Cx 43 within the specialized conduction system of the ventricle. Row 5: Sectional slides of the bundle branches (BB) demonstrating high levels of both Cx 40 and Cx 43 within the latter conduction system with the possibility of colocalization. (π) demarcates the lower nodal cell region.

Cx 45 immunolabeling sections were shown to demonstrate the isolation of Cx 40 within the packed mid node. Blue staining indicates connective tissue while red staining indicates myocardial cells.

TC

Cx 40

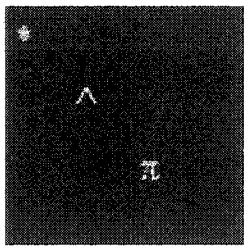

Cx 43

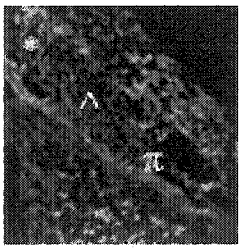

Cx 45

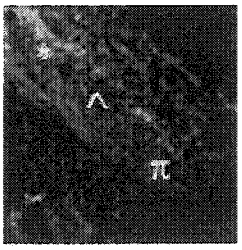

PMNC

Cx 40

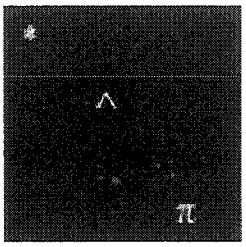

Cx 43

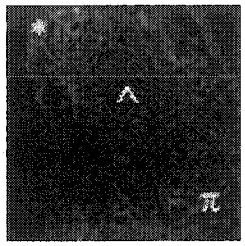

Cx 45

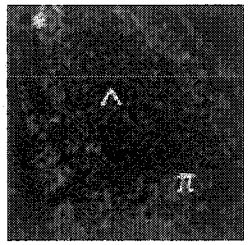

DMNC

Cx 40

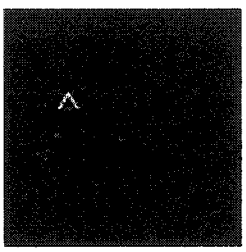

Cx 43

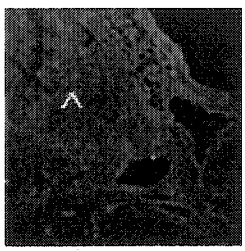

Cx 45

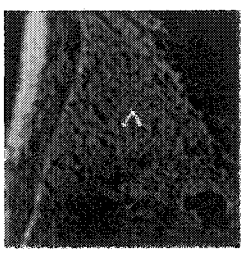

BHis

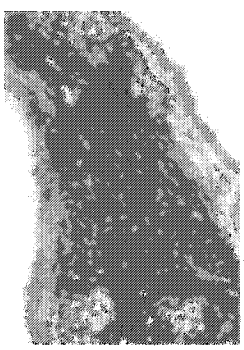

Cx 40

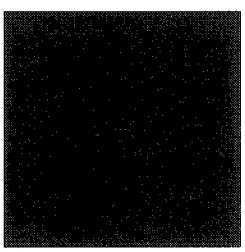

Cx 43

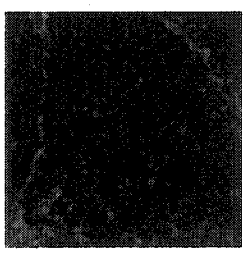

Cx 45

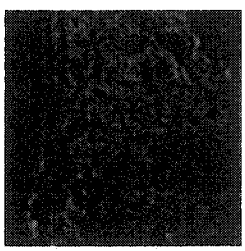

BB

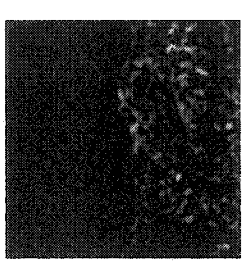

Cx 40

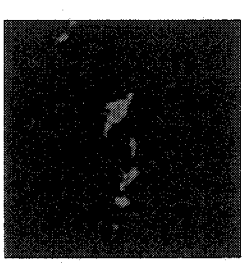

Cx 43

40/43

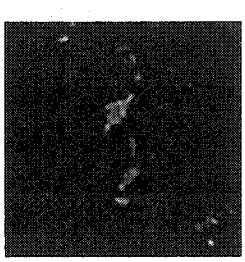

The packed mid nodal cells of the AV node (Fig 5, Rows 2 & 3) displayed the converse of the transitional cells. Within this area no levels of Cx 43 immunofluorescence were seen, however, Cx 40 immunolabeling was clearly evident. Also, the distribution of Cx 40 within the proximal ventricular specialized conduction system (Fig 5, Row 4) is isolated. There was no evidence of commingling between Cx 40 and Cx 43 within the bundle of His and the proximal bundle branches (Fig 5, Row 5). However, within the distal arm of the bundle branch there was evidence of intermingling and possible colocalization. However, recent studies have demonstrated that Cx 40 and Cx 43 do not from heteromeric channels[34]. Therefore, it is most likely that the two proteins are in extreme proximity with one another in distal portions of the bundle branches.

Electrophysiology

The conduction time across the rabbit AV node has been an area of particular interest for some time. In order to observe the conduction time and the rate-induced changes that occur across the AV node a periodic premature pacing protocol[35] is used. Fig 6 is a schematic representation of the rabbit AV node and the placement of the stimulating (S) electrode, the atrial (A) recording electrode and the His (H) recording electrode. Due to the close proximity of the stimulating and atrial electrodes our temporal recordings for the atrium were taken at 4ms after the beginning of the 8ms stimulating pulse. Therefore, as seen in Fig 7, S represents the stimulating pulse and is synonymous with A (Fig 8), the H0 following S0 represents the recording at the His. S1 and H1 represent the stimulating and His recordings of the premature beat, respectively.

Figure 6

Schematic representation of the positioning of the stimulating electrode, atrial and His recording electrodes around the triangle of Koch, bordered by the tendon of Todaro (TT), coronary sinus (CS) and the annulus fibrosus (AF). S (blue lines) represents the bipolar stimulating electrode. H (red lines) represents the bipolar His recording electrode. A (black lines) represents the bipolar atrial recording electrode.

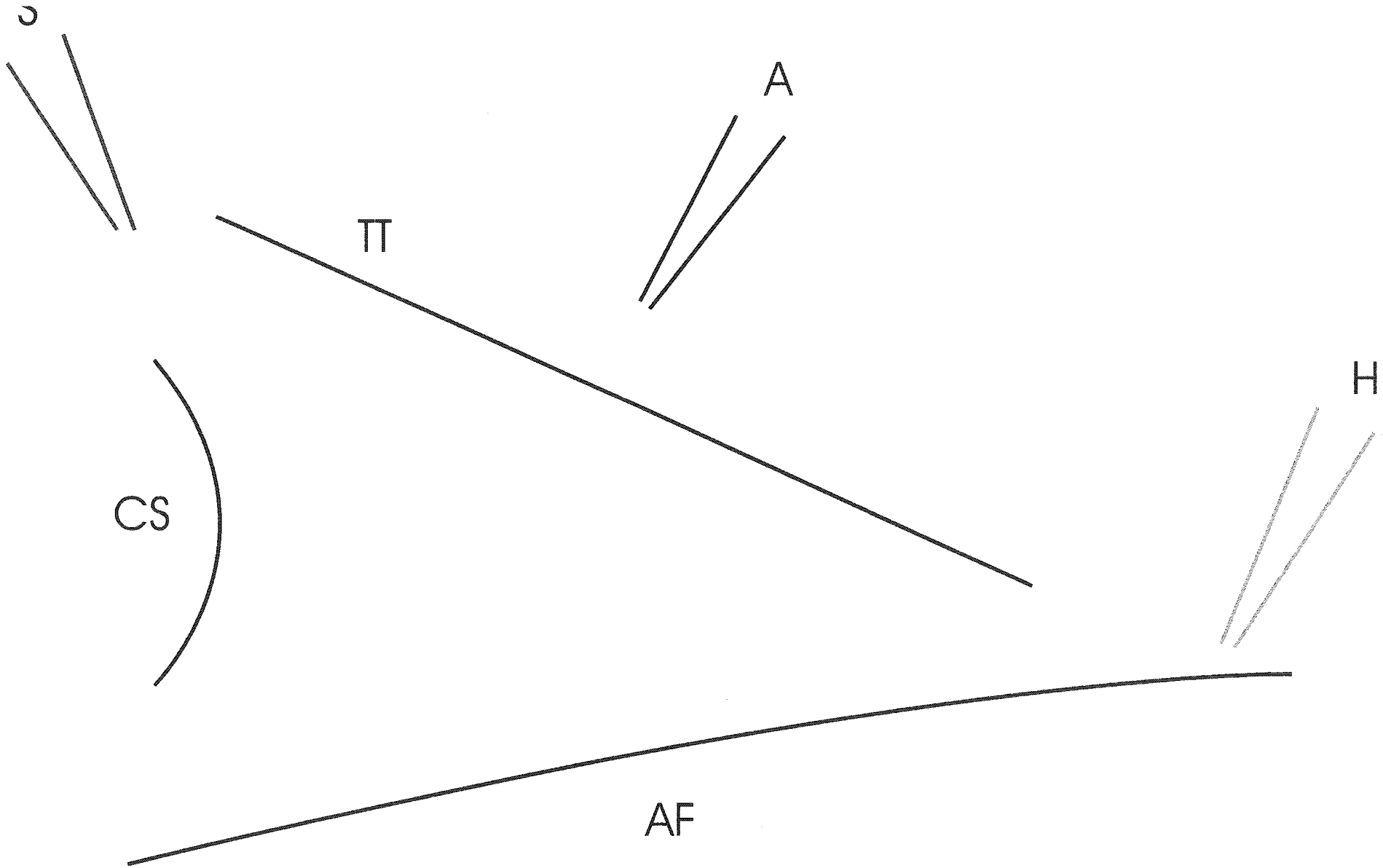
S
A
TT
H
CS
AF

Figure 7

Electrical recordings taken from the rabbit AV node during a premature pacing protocol. S0 and H0 represent the recordings during basic pacing cycle. S1 and H1 represent the recording from the premature beat. S2 and H2 represent the recording from the rate-induced change beat. The numerical values on the Y-axis were arbitrary values assigned by the data analysis program.

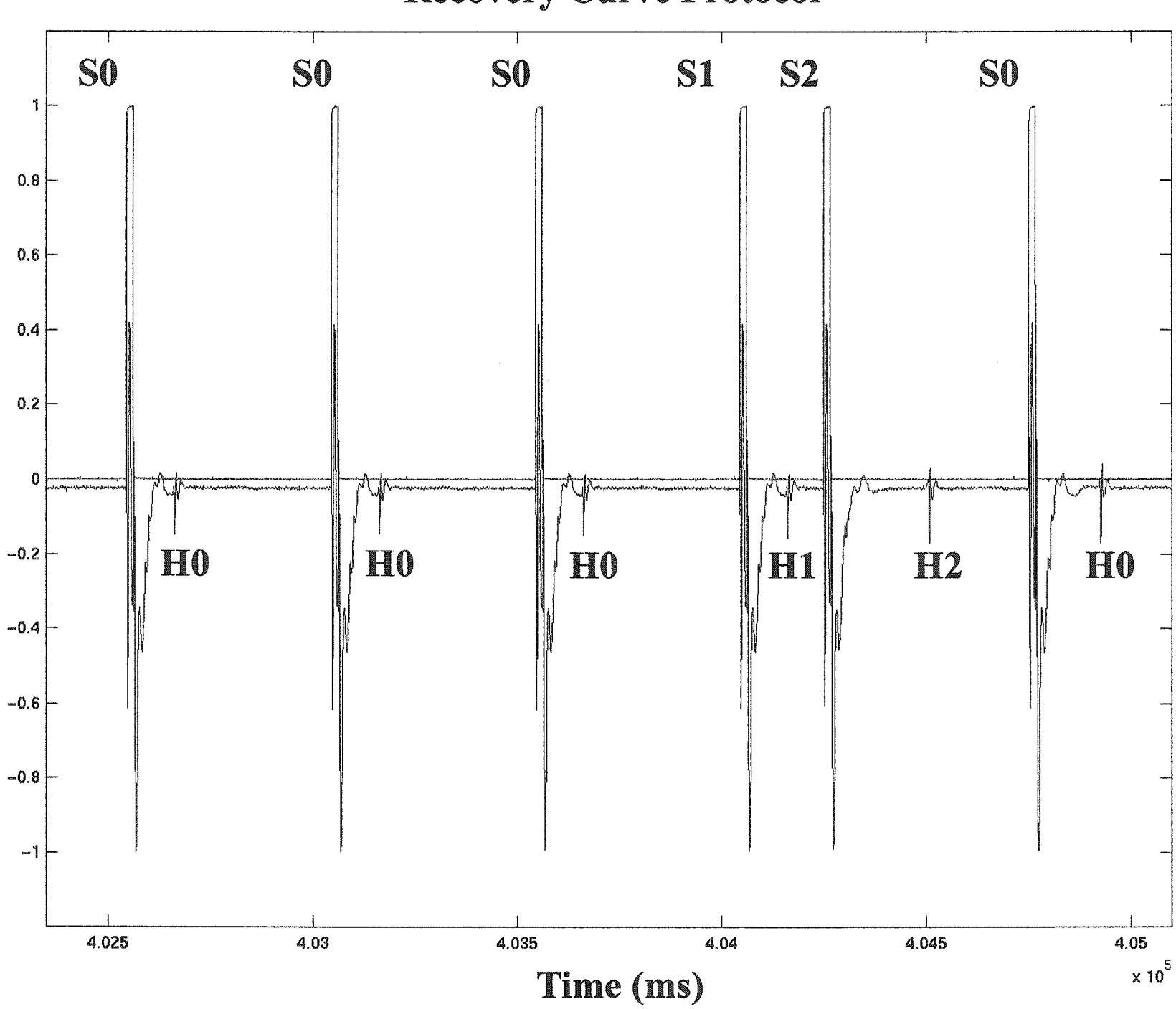
Recovery Curve Protocol
S0
S0
S0
S1
S2
S0
H0
H0
H0
H1
H2
H0
1
0.8
0.6
0.4
0.2
0
−0.2
−0.4
−0.6
−0.8
−1
4.025
4.03
4.035
4.04
4.045
4.05
Time (ms)
x 10^5

Figure 8

Effects of di-4-ANEPPS on the nodal recovery curve. (=) represents the data obtained from the pacing protocol performed on the heart with the addition of 2,3-butanedione monoxime. (◊) represents the data obtained from the pacing protocol performed on the same heart with the further addition of 50 μM of di-4-ANEPPS.

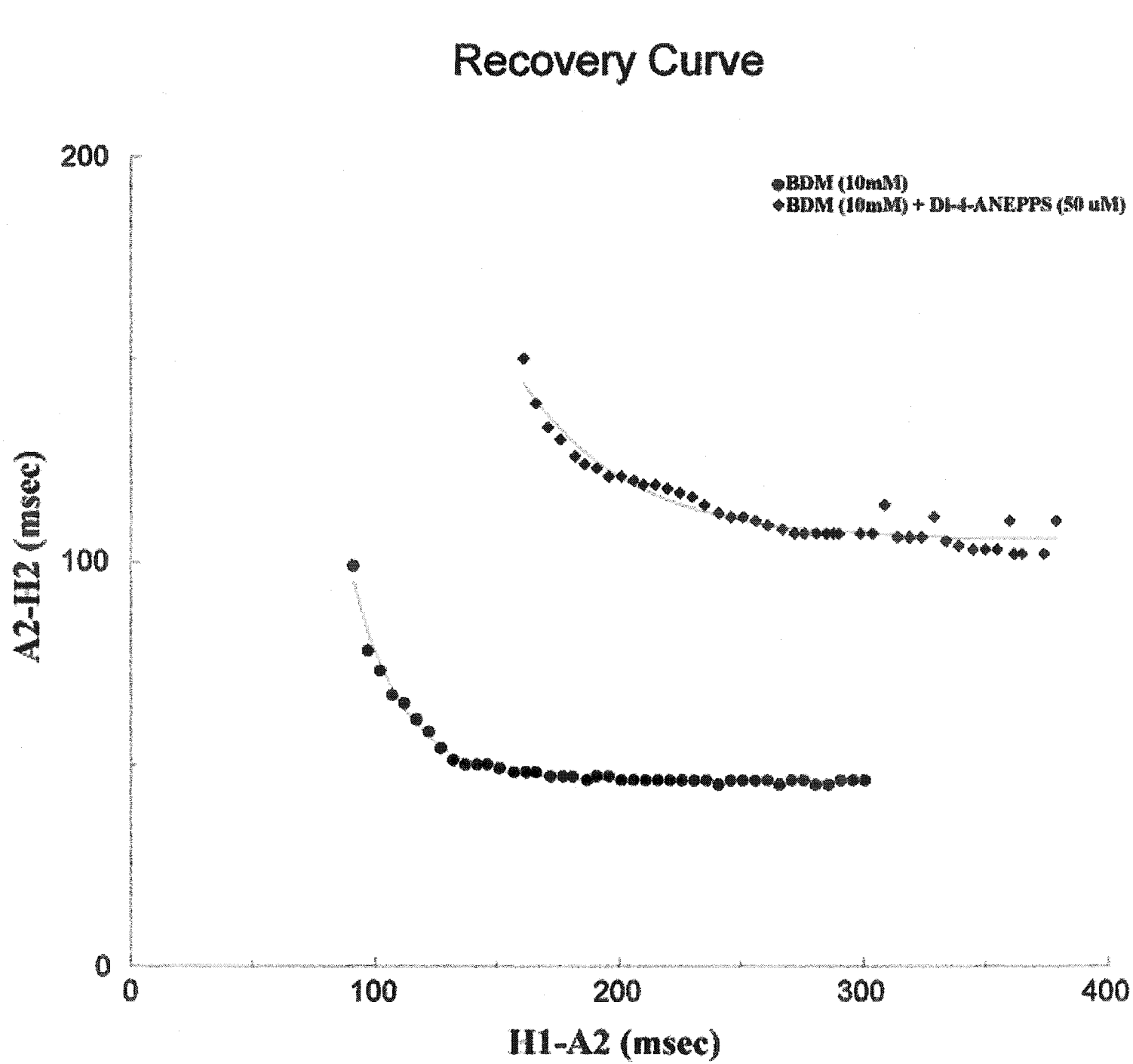
Recovery Curve
BDM (10mM)
BDM (10mM) + Di-4-ANEPPS (50 uM)
A2-H2 (msec)
H1-A2 (msec)
0
100
200
300
400

S2 and H2 represent the stimulating and His recordings of the rate-induced change caused by the premature beat.

Rate-induced prolongations and shortenings of the A2-H2 intervals are observed at long and short H1-A2 intervals, respectively[35]. The A2-H2 intervals recorded with the periodic premature stimulations of the atrium were plotted against the corresponding H1-A2 interval recordings (Fig 8) producing a recovery curve. This curve demonstrates the time that the node has to recover its excitability before the occurrence of another activation beat.

For our study, the control recovery curve was the one resulting from a periodic premature pacing protocol performed on a rabbit heart that was subjected to the contraction artifact reducer, butanedione monoxime (BDM). Previous studies have shown that the addition of BDM has no adverse effect on rabbit AV node conduction[36]. The same pacing protocol was performed on the same heart after a 30 min superfusion of di-4-ANEPPS. The resulting recovery curve shows a shift up and to the right demonstrating that the voltage-sensitive dye does have an inhibitory effect on both the conduction and recovery times on the rabbit AV node. This observation was not surprising in that di-4-ANEPPS causes photodynamic toxicity to isolated cardiomyocytes[37].

Optical Mapping

High-resolution optical mapping of the rabbit AV node is an area of intense interest in the pursuit to understand the electrophysiology of the AV node. The most appreciated advantage of this technique becomes most apparent when attempting to map the spread of activation through the node. Of course, this technique depends on the use of

many tools such as a cooled CCD camera, excitation and emission filters, voltage sensitive dyes and a recording device. Figure 9 is a schematic representation of the set up that was designed and constructed for this study.

Once the rabbit heart has been dissected (Fig 10), pinned in place in the preparation chamber, loaded with both BDM and di-4-ANEPPS optical recordings can be made of the propagational wave patterns through the AV node (Fig 11). Figure 12 illustrates the individual optical signals recorded from this preparation during the propagation of a single atrial beat. It is apparent that the optical signal becomes more pronounced when moving from the input into the AV node (on the left) to the output (on the right).

However, what is most noticeable with these recordings is the obvious prolonged activity that occurs at the area near the central fibrous body. This is the exact location of the mid-node region of the AV node. Since our sampling rate was performed at 100 frames/second, each frame represents a 10ms difference from its neighbour. Therefore, the entire conduction time across the node was approximately 110ms (which corresponds to the BDM and di-4-ANEPPS recovery curve (◊) from Fig 8). Of this 110 ms, ~ 40 ms is due to this phenomenon of prolonged activity. The temporal resolution of our system is sufficient for resolving the slow conduction through the AV node. However, the detailed time course of conduction across faster tissue, such as atrial and ventricular myocardium, was not possible.

Figure 9

Schematic representation of the optical recording device and tandem-lens system. CCD: Charged Couple Device.

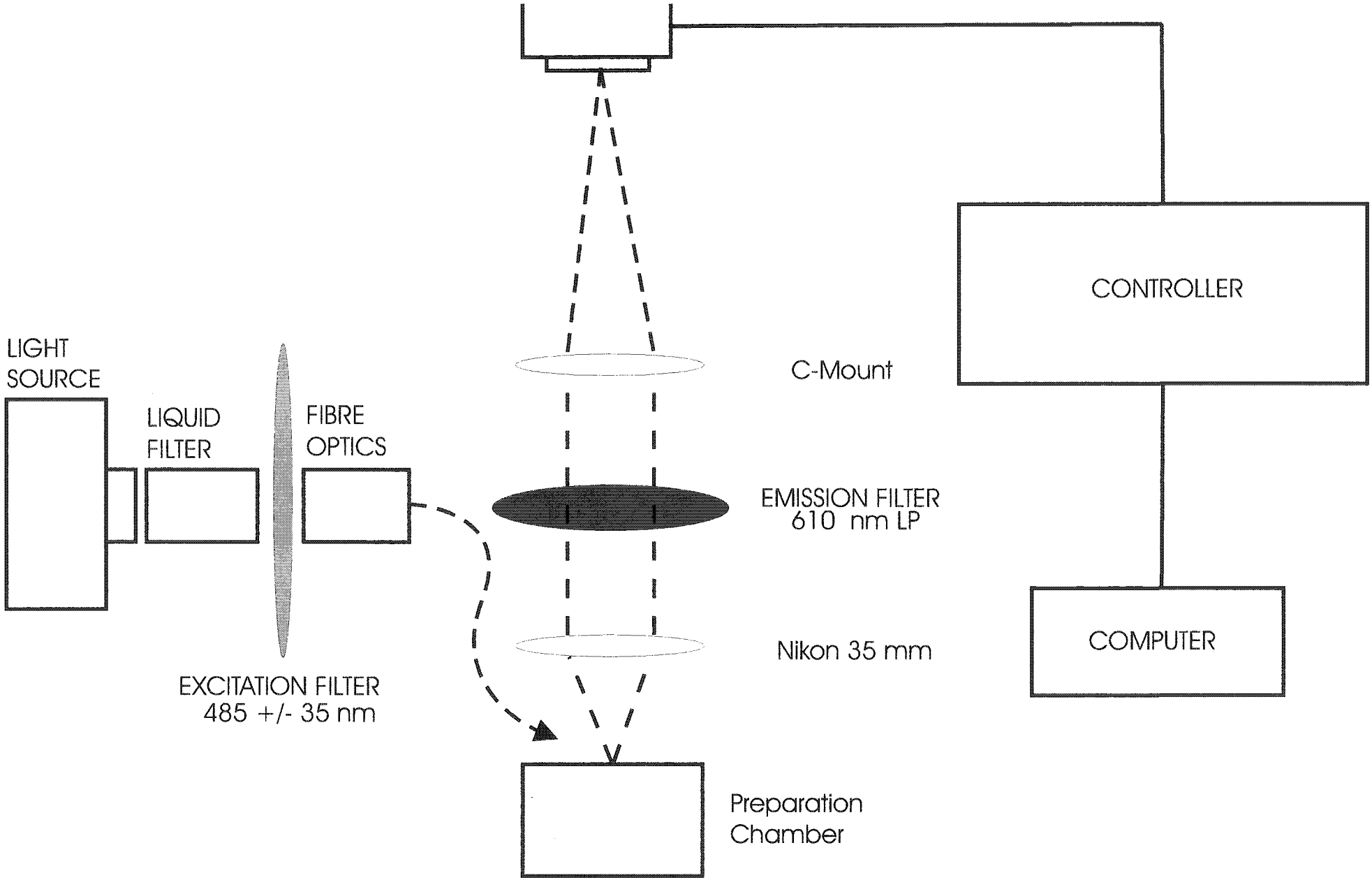
LIGHT
SOURCE
LIQUID
FILTER
FIBRE
OPTICS
EXCITATION FILTER
485 +/- 35 nm
C-Mount
EMISSION FILTER
610 nm LP
Nikon 35 mm
Preparation
Chamber
CONTROLLER
COMPUTER

Figure 10

Dissected preparation (rabbit heart) exposing the superficial surface of the AV node. tT: tendon of Todaro; CS: coronary sinus; CFB: central fibrous body; fRA: flap of the right atrium. This was the preparation used for the electrophysiological (Fig 7) as well as the optical (Fig 12) recordings.

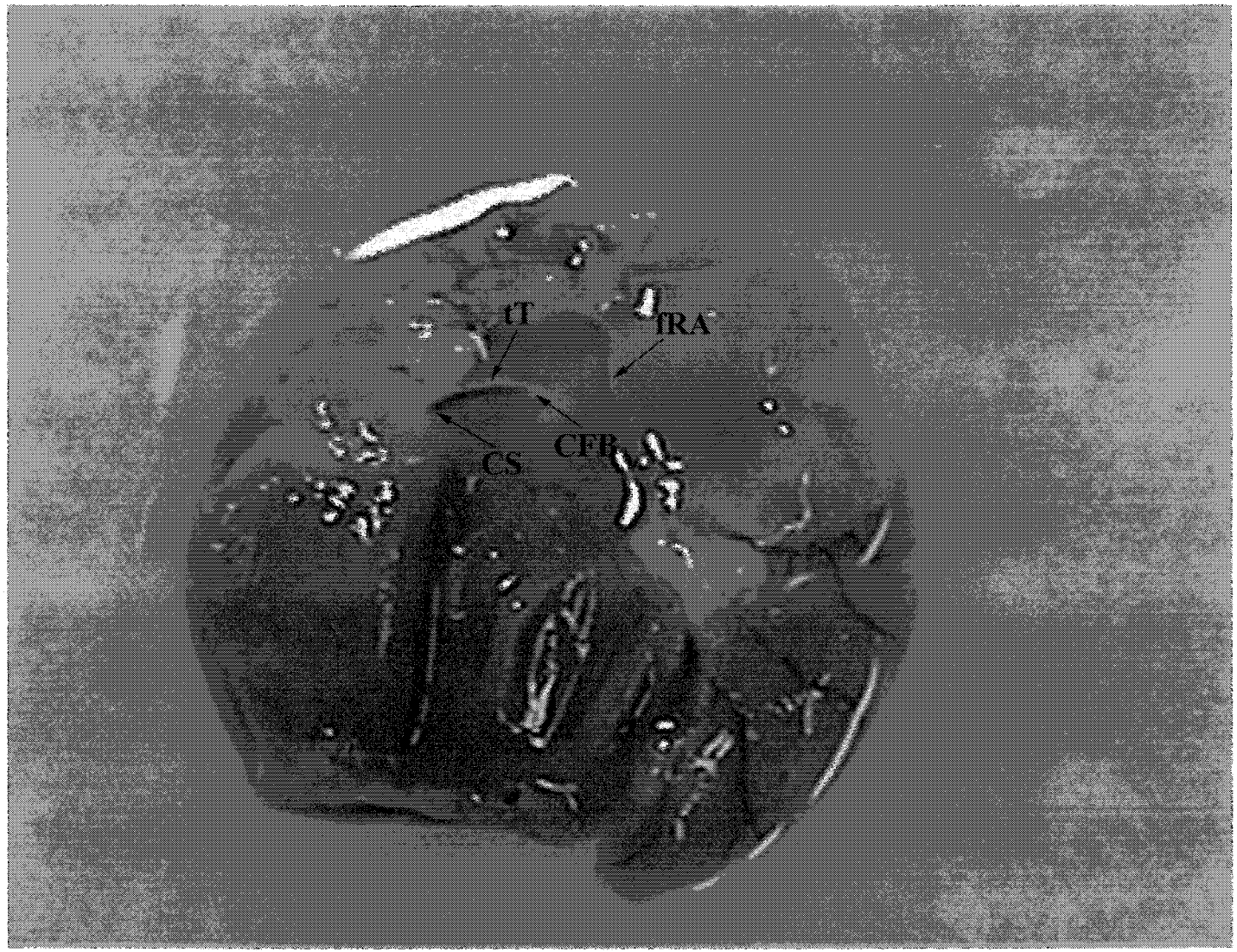
tT
TRA
CS
CFB

Figure 11

Single frame image recorded from the CCD of the preparation. tT: tendon of Todaro; CS: coronary sinus; CFB: central fibrous body; fRA: flap of the right atrium. ~10X magnification.

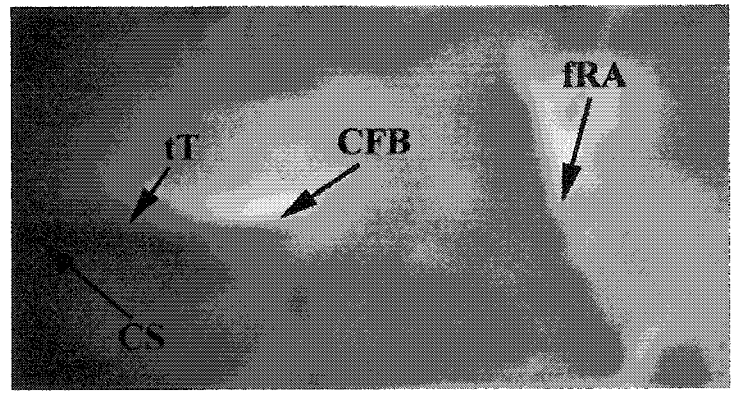
fRA
fT
CFB
CS

Figure 12

Optical recordings of the propagation wave through the AV node during a single heartbeat. The recordings have been superimposed over the same single image from figure 11. Blue represents low electrical activity, red represents high electrical activity. Arrow represents the directional reading of the figure, left to right; top to bottom. Note the prolonged activity in frames 10-13. ~7X magnification.

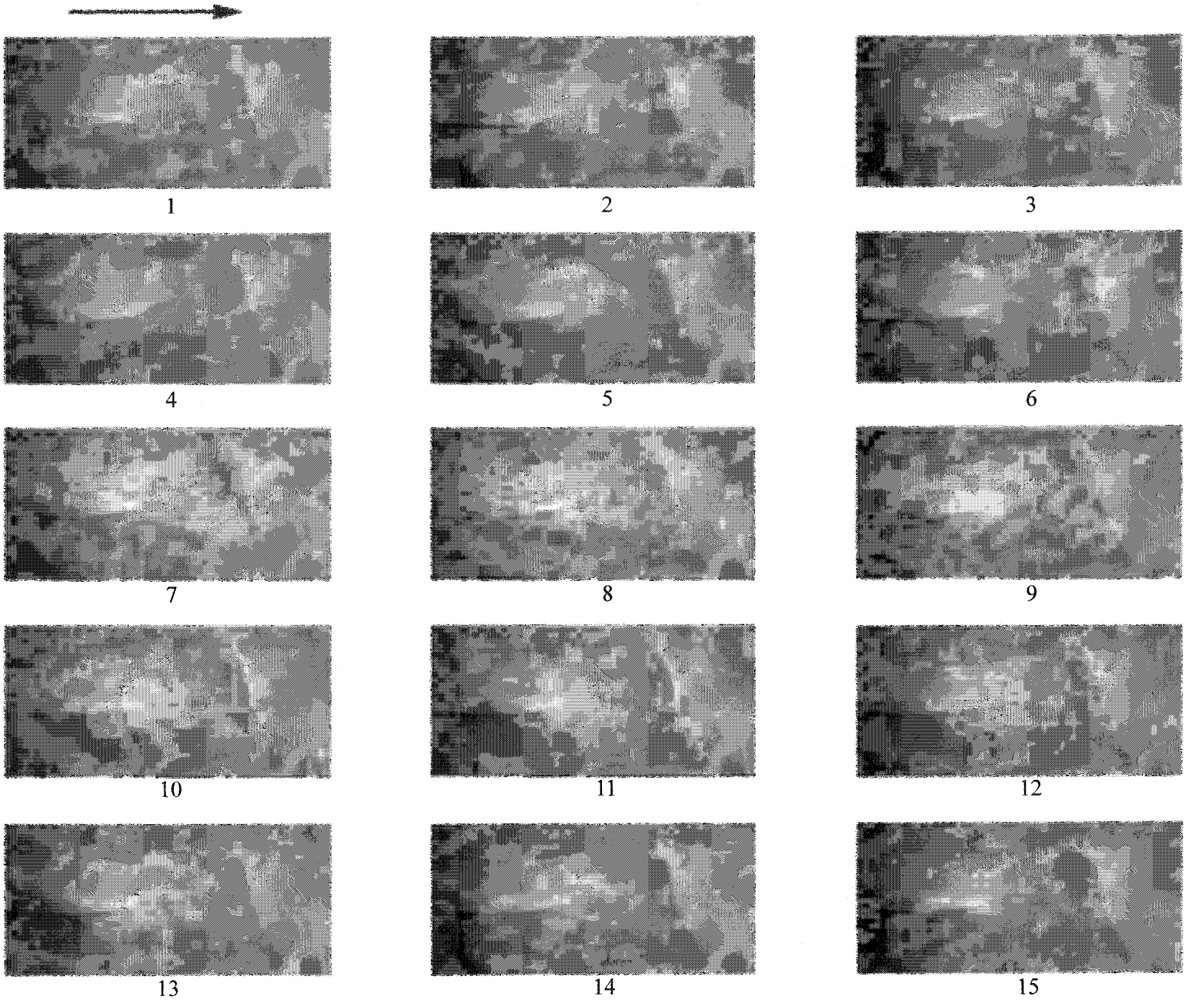
1
2
3
4
5
6
7
8
9
10
11
12
13
14
15

CHAPTER 4

DISCUSSION

It has been suggested that the slow impulse propagation through the mid-node is partly due to the absence of sodium channels in this region[40]. This absence can diminish the rapid upstroke component of an action potential[11] thereby causing a delay. It has also been suggested that due to the poor electrical coupling between the cells of the mid-node that the slow propagation in this region may also be due to the slowed intercellular diffusion of ions[39].

Of course, the pathway of propagation through the AV node has not yet been determined. However, it has been speculated that due to the higher levels of sodium channels and Cx 43 expression in the circumferential transitional cells, that the preferred pathway of propagation may be through the enveloping layer of cells surrounding the mid-node rather than through it[11]. Also suggesting that the mid-node may act as an electrical sink causing the slowed propagation. However, these and other studies have not yet determined whether the greatest delay within the AV node occurs between the transitional and mid-nodal cells or the mid-nodal and lower nodal cells.

With the combination of histological, immunohistochemical, electrophysiological and optical techniques this present study provides some insight into the question of the AV nodal delay. Although the specific expression of certain connexin (mainly Cx 40 and Cx 43) proteins within the cellular boundaries of the AV node have been reported[11,38,39], these studies did not demonstrate entirely the specific cellular regions within which each connexin protein were localized. Our study combined the histological background of the AV node with specific antibody staining to illustrate the localization of Cx 40 and Cx 43 within these cellular regions.

The Cx 40 antibody used in this study was prepared in rabbit against a GST fusion protein containing most of the unique C-terminal regions of rat Cx 40. The mid-nodal cells of the AV node were the only cells of the AV node that expressed Cx 40 at levels that were easily detected by immunoflourescence. The transitional and lower nodal cells showed a virtual absence of immunolabeling for Cx 40. The levels of Cx 40 expression in the bundle of His and upper regions of the bundle branches of the conduction system were exclusive as well.

The Cx 43 antibody was a synthetic peptide, prepared in mouse, corresponding to positions 252-270 of the native sequence from rat cardiac Cx 43. The transitional and lower nodal cells showed a relatively high level of immunolabeling for Cx 43. The circumferential cells also showed levels of immunolabeling however; the intensity was less obvious due to the sporadic nature of the cells of this region. Cx 43 expression was apparent at other levels of the conduction system mainly the lower regions of the bundle branches. Due to the concerns around the purity of the cDNA corresponding for Cx 45 and the possibility for cross-reactivity of the two Cx 45 antibodies, Cx 45 immunolabeling was used as a control in our study. The lack of immunolabeling of Cx 45 within the mid-node further demonstrated the isolation of Cx 40 within this region.

The combination of extracellular electrodes, a high-resolution optical recording device and a voltage-sensitive dye allowed us to successfully map the propagational wave of an atrial beat through the AV node and locate the region of the functional delay within the AV node. The propagational wave from the atria enters the AV node at the area of the ostium of the coronary sinus. The wave passes through the transitional cells, traverses the AV node and exits through the lower nodal cells into the bundle of His. It is at the

region of the mid-node that the functional delay is most apparent using the optical recording technique. With each propagational wave, there is an area of prolonged activity at this region.

One possible explanation for this phenomenon is that due to the variable thickness of the AV node this prolonged activity is due to the later depolarization of the deeper nodal cells[31]. However, we have shown that there is a distinct boundary between cellular regions of the AV node expressing Cx 43 and Cx 40. As mentioned previously, the surrounding cells of the mid-node express Cx 43 whereas the cells within the mid-node express Cx 40. Therefore, this phenomenon may possibly be due to the delay between the electrical interaction of these particular areas of the AV node during an atrial beat.

Recent studies have demonstrated that Cx 40 and Cx 43 do not form heteromeric channels[34]. However, it may be that the neighbouring mid-nodal and circumferential cells display an unusual property in that they express both Cx 40 and Cx 43. This unique method of communication may contribute in the functional delay along with the aforementioned properties within this region of the AV node.

REFERENCES

1. Coraboeuf, E., Weidmann, S. Potentiels d'action du muscle cardiaque obtenues a l'aide de microelectrodes intracellulaires. Presence d'une inversion de potentiel. *C.R. Soc. Biol.* **143**: 1360-1361, 1949.
2. Tawara. S. *Das Reizleitungssystem des Herzens.* Jena, Germany: Fischer, 1906.
3. Wenckebach, K., Winterberg, H. *Die Unregelmässige Herztätigkeit.* Leipzig, Germany. Engelmann, 1927
4. Draper, M.H., Weidmann, S. Cardiac resting and action potentials recorded with an intracellular electrode. *J. Physiol. (Lond.)* **115**: 74-94, 1951.
5. Vasalle, M. The relationship among cardiac pacemakers. Overdrive suppression. *Circ. Res.* **41**: 269-277, 1977.
6. Koch, W. Weitere Mitteilungen ueber den Sinusknoten des Herzens. *Verh. Dtsch.Ges. Pathol.* **13**: 85-92, 1909.
7. Anderson, R. H. Histologic and histochemical evidence concerning the presence of morphologically distinct cellular zones within the rabbit atrioventricular node. *Anat. Rec.* **173**: 7-24, 1972.
8. Petrecca, K., Shrier, A. Spatial distribution of nerve processes and β-adrenoreceptors in the rat atrioventricular node. *J. Anat.* **192**: 517-528, 1998.
9. Anderson, R.H., Janse, M.J., van Capalle, F.J.L., Billette, J., Becker, A.E., Durrer, D. A combined morphological and electrophysiological study of the atrioventricular node of the rabbit heart. *Circ. Res.* **35**: 909-922, 1974.
10. Meijler, F.L., Janse, M.J. Morphology and electrophysiology of the mammalian atrioventricular node. *Physical Reviews* **68**: 608-639, 1988.
11. Petrecca, K., Amellal, F., Laird, D.W., Cohen, S.A., Shrier, A. Sodium channel distribution within the rabbit atrioventricular node as analysed by confocal microscopy. *J. Physiology* **501.2**: 263-274, 1997.
12. Hoffman, B.F., Paes de Carvalho, A., de Mello, W.C. Transmembrane potentials of single fibres of the atrioventricular node. *Nature* **181**: 66-67, 1958.
13. Mazgalev, T., Dreifus, L.S., Iinuma, H., Michelson, E.L. Effects of the site and timing of atrioventricular nodal input of atrioventricular conduction in the isolated perfused rabbit heart. *Circulation* **70**: 748-759, 1984.
14. Paes de Carvahlo, A., de Almeida, D.F. Spread of activity through the atrioventricular node. *Circ. Res.* **8**: 801-809, 1960.
15. Robertson, J.D. The occurrence of a subunit pattern in the unit membranes of club endings in mauthner cell synapses in goldfish brains. *J. Cell Biol.* **19**: 201-221, 1963.
16. Bruzzone, R., White, T. W., Paul, D. L. Connections with connexins: the molecular basis of direct intercellular signaling. *Eur. J. Biochem.* **238**: 1-27, 1996.
17. Paul, D.L. Molecular cloning of cDNA for rat liver gap junction protein. *J. Cell Biol.* **103**: 123-134.
18. Zimmer, D.B., Green, C.R., Evans, W.H., Gilula, N.B. Topological analysis of the major protein in isolated intact rat liver gap junctions and gap junction-derived single membrane structures. *J. Biol. Chem.* **262**: 7751-7763, 1987.

19. Hoh, J.H., John, S.A., Revel, J.P. Molecular cloning and characterization of a new member of the gap junction gene family, connexin-31. *J. Biol. Chem.* **266**: 6524-6531, 1991.
20. Gros, Daniel, Jarry-Guichard, T., Ten Velde, I., de Maziere, A., van Kempen, M., Davoust, J., Briand, J., Moorman, A., Jongsma, H. Restricted distribution of connexin 40, a gap junctional protein, in mammalian heart. *Circ. Res.* **74(5)**: 839-851, 1994.
21. Van Kempen, M., Fromaget, C., Gros, D., Moorman, A., Lamers, W. Spatial distribution of connexin 43, the major cardiac gap junction protein, in the developing and adult rat heart. *Circ. Res.* **68**: 1638-1651, 1991.
22. Gourdie, R., Green, C., Severs, N. Thompson, R. Immunolabeling patterns of gap junction connexins in the developing and mature rat heart. *Anat. Embryol.* **185**: 363-378, 1992.
23. Burt, J., Spray, D. Single-channel events and gating behavior of the cardiac gap junction channel. *Proc. Natl. Acad. Sci. USA* **85**: 3431-3434, 1988.
24. Hulser, D., Eckert, R., Zempel, G. Rottler, R. Biophysical and biochemical characterization of gap junction channels in cultured mammalian cells. In: Communication at the workshop on cellular networks; Sept 1992; Palanga, Lithuania.
25. Coppen, S., Kodama, I., Boyett, M., Bobrzynski, H., Takagishi, Y., Honjo, H., Yeh, H., Severs, N. Connexin45, a major connexin of the rabbit sinoatrial node, is co-expressed with connexin43 in a restricted zone at the nodal-crista terminalis border. *J. Hist. Cyto.* **47(7)**: 907-918, 1999.
26. Coppen, S., Dupont, E., Rothery, S., Severs, N. Connexin45 expression is preferentially associated with the ventricular conduction system in mouse and rat heart. *Circ. Res.* **82**: 232-243, 1998.
27. Billette, J. Atrioventricular nodal activation during periodic premature stimulation of the atrium. *Am. J. Physiol.* **252**: H163-H177, 1987.
28. Fast, V.G., Kleber, A.G. Microscopic conduction in cultured strands of neonatal rat heart cells measured with voltage-sensitive dyes. *Circ. Res.* **73**: 914-925, 1993.
29. Ratzlaff, E.H., Grinvald, A. A tandem-lens epifluorescence macroscope: hundred-fold brightness advantage for wide-field imaging. *J. Neuro. Meth.* **36**: 127-137, 1991.
30. Efimov, I.R., Fahy, G.J., Cheng, Y.N., Van Wagoner, D.R., Tchou, P.J., Mazgalev, T.N. High resolution fluorescent imaging of rabbit heart does not reveal a distinct atrioventricular nodal anterior input channel (fast pathway) during sinus rhythm. *J. Cardiovasc. Electrophysiol.* **8**: 295-306, 1997.
31. Efimov, I.R., Mazgalev, T.N. High resolution, three-dimensional fluorescent imaging reveals multilayer conduction pattern in the atrioventricular node. *Circ.* **98**: 54-57, 1998.
32. Choi, B., Salama, G. Optical mapping of atrioventricular node reveals a conduction barrier between atrial and nodal cells. *Am. J. Physiol.* **274**: H828-H845, 1998.
33. Coppen, S.R., Dupont, E., Rothery, S., Severs, N.J. Connexin45 expression is preferentially associated with the ventricular conduction system in mouse and rat heart. *Circ. Res.* **82**: 232-243, 1998.

34. He, D. S., Jiang, J. X., Taffet, S.M., Burt, J. M. Formation of heteromeric gap junction channels by connexins 40 and 43 in vascular smooth muscle cells. *Proc. Natl. Acad. Sci.* **96**: 6495-6500, 1999.
35. Billette, J, St-Vincent, M. Functional origin of rate-induced changes in atrioventricular nodal conduction time of premature beats in the rabbit. *Can. J. Physiol. Pharmacol.* **65**: 2329-2337, 1987.
36. Cheng, Y., Mowrey, K., Efimov, I., Van Wagoner, D., Tchou, P., Mazgalev, T. Effects of 2,3-butanedione monoxime on the atrial-atrioventricular nodal conduction in isolated rabbit heart. *J. Cardiovasc. Electrophysiol.* **8**: 790-802, 1997.
37. Schaffer, P., Ahammer, H., Muller, W., Koidl, B., Windisch, H. Di-4-ANEPPS causes photodynamic damage to isolated cardiomyocytes. *Pflugers Arch.* **426**: 548-551, 1994.
38. Gourdie, R. The map of the heart: gap junctions, connexin diversity and retroviral studies of conduction myocyte lineage. *Clin. Sci.* **88**: 257-262, 1995.
39. Gourdie, R., Severs, N., Green, C., Rothery, S., Germroth, P., Thompson, R. The spatial distribution and relative abundance of the gap-junctions connexin40 and connexin43 correlate to functional properties of the cardiac conduction system. *J. Cell Sci.* **105**: 985-991, 1993.
40. Munk, A., Adjemian, R., Zhao, J., Ogbaghebriel, A., Shrier, A. Electrophysiological properties of morphologically distinct cells isolated from the rabbit atrioventricular node. *J. Physiolo.* **493**: 801-818, 1996.